point is characterized by the following parameters: $\alpha \sim 1.72$, Re = 21,600. The viscous-type neutral curves for $\beta = 0$ and 0.09 are illustrated in Fig. 4 (curves 0 and 1).

The author expresses his gratitude to V. N. Shtern for his attention to this research and discussion of the results.

LITERATURE CITED

1. T. A. Vil'gel'mi and V. N. Shtern, "The stability of a spiral flow between adjacent cylinders," Izv. Akad. Nauk SSSR, Mekh. Zhidk. Gaza, No. 3, 35-44 (1974).
2. J. Kaye and E. C. Elgar, "Modes of adiabatic and diabatic fluid flow in an annulus with an inner rotating cylinder," Trans. ASME, 80, No. 3, 753-765 (1958).
3. V. I. Yudovich, "Secondary flows and the instability of a fluid between rotating cylinders," Prikl. Mat. Mekh., 30, No. 4, 688-698 (1966).
4. I. P. Andreichikov and V. I. Yudovich, "Self-oscillating modes branching off from a Poiseuille flow in a two-dimensional channel," Dokl. Akad. Nauk SSSR, 202, No. 4, 791-793 (1972).
5. V. I. Yudovich, "The origin of self-oscillations in a fluid," Prikl. Mat. Mekh., 35, No. 4, 638-655 (1971).
6. M. A. Gol'dshtik and V. A. Sapozhnikov, "The stability of the flow in an annular channel," Izv. Akad. Nauk SSSR, Mekh. Zhidk. Gaza, No. 4, 102-109 (1971).

AN OPTICAL METHOD FOR INVESTIGATING THE MICROSTRUCTURE OF TURBULENT FLOW

É. G. Goncharov, L. G. Kovalenko, and É. I. Krasovskii

UDC 535.411:551.463

In a number of cases the study of the structure of small-scale high-intensity turbulence shows a deviation from Taylor's hypothesis which is manifested in incompatible values of time and spatial correlations [1]. In view of this the spatial structure of the flow cannot be estimated from a measurement of the autocorrelation of processes recorded by point transducer such as the various types of anemometers widely used to study turbulence. In this case it becomes important to use instruments with an analyzing volume larger than the microscale of the phenomenon under study and methods enabling one to record the state of a chosen volume at a certain instant with the simultaneous visualization of the flow. In particular, this metho was used in [2] for the quantitative determinations of certain characteristics of turbulence by introducing tracer particles into the medium and recording their distribution through the volume photographically. In many cases shadow optical instruments [3, 4] are used for the visualization of optical inhomogeneities in transparent media. Their use has a number of advantages over visualization methods employing finely dispersed materials or dyestuffs, since they avoid inertial effects which always accompany the introduction of tracer particles

We examine certain problems of the statistical analysis of flow domains whose dimensions are determined by the diameter of the light beam of the shadow instrument. Since the recorders used in investigating the microstructure of these domains are at best two-dimensional, whereas the field parameter being measured is a multidimensional quantity, it must be established how this affects the nature of the statistical field data being measured. One of the fundamental characteristics of a field is its wave-number power spectrum $g(\bar{k})$, in certain cases called the Wiener spectrum, and by analogy with one-dimensional processes having the meaning of the average variance of the spectral components with spatial frequencies in a small interval around $\bar{k}$ divided by the size of this interval. The use of measuring devices having a dimensionality smaller than that of the field being measured is equivalent to the effect of spectral windows which change the characteristics of the estimate of the spectrum. The dimensionality of a spectral window corresponds to that of the recording device [5]. In other words, the width of a spectral window along one of the frequency coordinates is inversely proportional to the sample length with respect to the corresponding spatial or time coor-

Leningrad. Translated from Zhurnal Prikladnoi Mekhaniki i Tekhnicheskoi Fiziki, No. 6, pp. 78-83, November-December, 1978. Original article submitted May 25, 1977.

dinate. For example, the field $\varepsilon_{t_0}(x, y, z)$ is a spatial cross section of the field $\varepsilon(x, y, z, t)$ at time t_0. The reduction of the dimension of the realization corresponds to the introduction of a delta function in the time coordinate. Then a cross section of the field has the form

$$\varepsilon(x, y, z, t_0) = \varepsilon(x, y, z, t)\,\delta(t - t_0) = \varepsilon_{t_0}(x, y, z).$$

In this case, an increase in the width of the spectral window along this coordinate corresponds to the integration of the complete spectrum with respect to the time frequency. Thus, the analysis of the spectrum of a cross section of the field can be considered as the analysis of the projection of the spectrum on the f axis:

$$g_f(p, q, r) = \int_{-\infty}^{\infty} g(p, q, r, f)\,df.$$

The recorders used in optical instruments are either photoelectric detectors or two-dimensional devices based on the recording of the distribution of illumination over a photosensitive layer. In the latter case we are concerned with the projection of a spatial cross section of the field on a plane, for example, the xz plane, which can be thought of as the Fourier transform with respect to y for a zero value of the frequency q:

$$\varepsilon_{yt_0}(x, z) = \int_{-\infty}^{\infty} \varepsilon_{t_0}(x, y, z)\; e^{-j\cdot 2\pi\cdot 0\cdot y}\,dy. \tag{1}$$

Thus, the integration of the realization is equivalent to the Fourier transform of the spatial cross section with zero values of the spatial frequencies corresponding to the coordinate over which the integration is performed. The Fourier transform of the projection of the field $\varepsilon_{yt_0}(x, z)$ is the two-dimensional Fourier spectrum of the projection of a spatial cross-section of the full-dimensional field and, taking account of (1), can be written in the form

$$\int_{-\infty}^{\infty}\int \varepsilon_{yt_0}(x, z)\, e^{-j2\pi(px+rz)}dxdz = \int\int_{-\infty}^{\infty}\int \varepsilon_{t_0}(x, y, z)\, e^{-j2\pi(px+0\cdot y+rz)}dxdydz = C(p, 0, r).$$

Hence, the Wiener spectrum is

$$g_f(p, 0, r) = M\left\{\lim_{XZ\to\infty}\frac{1}{XZ}|C(p, 0, r)|^2\right\}. \tag{2}$$

Because of the integration, the spectral window can move only in the pr plane in frequency space. The width Δq of the window is inversely proportional to the length of the integration interval or, in other words, the integration is equivalent to low-frequency filtering in the band Δq. In the terminology of [5], the frequency band Δq is called the analysis zone. Within the limits of the zone, the spectrum is measured by a band window whose shape is determined by the shape of the transducer aperture. The smoothing of the projection of the field of the transducer aperture with the transfer characteristic $W(p, r)$ is equivalent to weighting the cross section of the spectrum $g_f(p, 0, r)$:

$$g_f'(p, 0, r) = g_f(p, 0, r)\; W(p, r).$$

In general, the statistical structure of a turbulent field varies with time and space, i.e., the field is moving. If a projection of the field is recorded within the time interval Δt (for example, recording by a small area of the photocells), then since Δt is finite, a band of time frequencies ΔF corresponding to a finite range of absolute values of spatial frequencies is admitted. In other words, the spectral density of the field is different from zero only within a shell of finite thickness, and the field is degenerate.

The cross section of the spectrum of a nondegenerate field can be estimated by using an instrument with photographic recording. A set of cross sections obtained at various instants with a stationary transducer does not suffice to establish the complete spectrum of the field or to determine the direction of motion of the field, but does enable one to judge the nature of the motion of the field in a certain cross section.

According to (2), the determination of a cross section of the spectrum requires the calculation of the Fourier spectra of a number of sample records which are long enough ($XZ \to \infty$) so that each result obtained is determined by a set of uncorrelated values of the field. The Wiener spectrum is determined by averaging over an ensemble of squares of the absolute

magnitudes of the Fourier spectra in order to smooth out the differences in the spectra from the various sample records. Since the spatial integration with respect to y is extended over finite limits, and the averaging is performed over a certain finite set of samples N, an estimate of the running value of the spectrum is obtained:

$$\hat{g}_f(p, 0, r) = \frac{1}{N}\sum_{i=1}^{N}\frac{|C(p, 0, r)|^2}{XZ}.$$

Since the measurement of C(p, 0, r) by using two-dimensional spectrum analyzers is rather complicated and tedious, it is expedient to use single-channel instruments. To do this, it is necessary to match the dimensionality of the recorders and the projection of the field being studied by decreasing the sample record length with respect to one of the coordinates by employing long, narrow, slotted diaphragms to eliminate part of the two-dimensional sample.

Since single-channel recorders operate on a real time scale, it is necessary to perform a time scan of the projection of the field to estimate the spectrum. The power spectrum of the time signal g(ω) recorded as a result of the scan determines a one-dimensional cross section of the spectrum:

$$g(\omega) = Ag_f'(p, 0, 0). \tag{3}$$

To calculate the coefficient A we start with the well-known expression [6] relating the spectrum of the output signal to that of the input for a scanning speed v:

$$g(\omega) = \frac{1}{2\pi v}\int_{-\infty}^{\infty} g_f'(p, 0, r)\, K_\xi(p, 0, r)\, dr.$$

Here $K_\xi(p, 0, r)$ is the Fourier transform of a function of the form

$$K_\xi(\theta_1, 0, \eta_1) = \int_{-\infty}^{\infty}\int h(\theta, 0, \eta)\, h(\theta + \theta_1, 0, \eta + \eta_1)\, d\theta d\eta,$$

where h(θ, 0, η) is the pulse response of the scanning system. For scanning by a rectangular slit we have

$$g(\omega) = \frac{1}{2\pi v}\sin^2\left(\frac{pa}{2}\right)\Big/\left(\frac{pa}{2}\right)^2\int_{-\infty}^{\infty} g_f'(p, 0, r)\cdot\sin^2\left(\frac{rb}{2}\right)\Big/\left(\frac{rb}{2}\right)^2 dr, \tag{4}$$

where a and b are the dimensions of the slit.

If the scale of the projection of the field being investigated is appreciably smaller than the size of the slit along one of the coordinate directions, for example, z(b >> a), Eq. (4) is written in the form [7]

$$g(\omega) = \frac{c^2}{vb}\sin^2\left(\frac{pa}{2}\right)\Big/\left(\frac{pa}{2}\right)^2\cdot g_f'(p, 0, 0),$$

where c is the photoelectric constant. Then

$$A = \frac{c^2}{vb}\sin^2\left(\frac{pa}{2}\right)\Big/\left(\frac{pa}{2}\right)^2.$$

Starting from this, an expression can be written for the variance of a two-dimensional field under the assumption that $\sin^2(pa/2)/(pa^2/2) = 1$ in the range of frequencies being investigated [7]:

$$\sigma_T^2 = \frac{1}{(2\pi)^2}\int_{-\infty}^{\infty} g_f'(p\ \ 0, 0)\, dp = \frac{b}{2\pi c^2}\sigma^2,$$

where σ^2 is the variance of the time signal in the scan.

The procedure developed was used to investigate the motion of a random density field formed by the displacement of a cylinder in a fluid. It is known [8] that in this case the turbulent flow results from a turbulent boundary layer produced on the cylinder as the viscous fluid flows past it. The vortex structure of the motion in the turbulent flow is due to a fluctuating velocity field which produces a field of pressure fluctuations giving rise to a variation of the density of the fluid. The density field was studied with an IAB-451 device

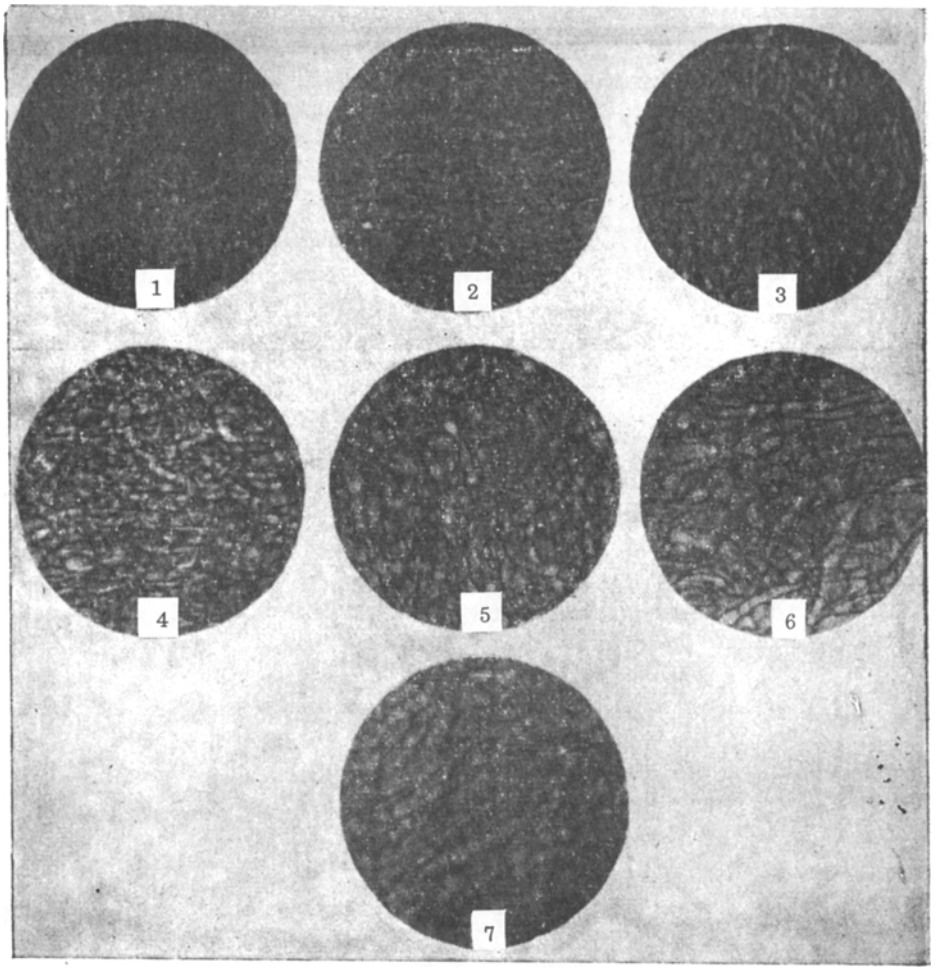

Fig. 1

connected to a camera for photographing the distribution of nonuniformities in the focal plane of the objective. The device was placed in special boxes at a certain depth below the surface of water. The volume being analyzed was contained between the light source and the photographic parts of the instrument and was illuminated with a parallel beam of light. The cylinder was displaced in this volume, and at successive instants of time photographs were taken of the distribution of inhomogeneities.

It should be noted that the flow pattern of the fluid obtained in the focal plane of the IAB-451 is characterized by a typical cell structure whose presence was pointed out in a number of papers [2, 9]. In particular, it was noted in [9] that the nature of the velocity and temperature distributions in an individual vortex cell could be judged from the shape and size of the cells. Information about the moving field was obtained from photographs of a number of projections of the field recorded at 10-sec intervals after the cylinder had reached the part of the device where the fluid was being analyzed. These photographs show the fluctuations of the transmission coefficient over the surface of the photosensitive layer (photographs 1-7 of Fig. 1). Then the fluctuations of the transmission coefficient were transformed into an electric signal [7] and the power spectral density of this signal was determined. Since the transmission coefficient is isotropically distributed over the surface of the photosensitive layer, a circular scan of the image of the diaphragm slit was performed.

The parameters of the apparatus were established by starting from the admissible value of the error [10]. For samples with an exponential correlation function, the bias of the estimate is of the order of 0.01 even for bandwidths of filter B, which are about half as large as the bandwidth of the process being investigated. Therefore, the choice of the filter bandwidth was determined by the admissible value of the variance of the estimate for a given sample record length T_r. The error for a finite value of BT_r was decreased by smoothing over an ensemble of N estimates for various portions of the image. Since for RC averaging the bias error is less than 0.02 for an averaging time of 4RC, the scan rate is determined

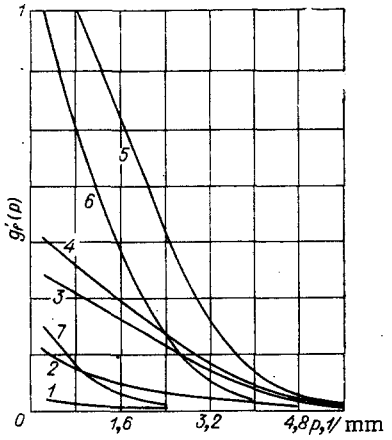

Fig. 2

as $R_s \leqslant B/4T_r$. In particular, for a scan rate of 0.1 Hz/sec the variance of the estimate is $\gamma = 0.3$ for $B = 40$ Hz and $T_r = 0.25$ sec. Smoothing over an ensemble of nine estimates reduced the variance of the estimate to 0.1.

Figure 2 shows cross sections of the spectrum of a smoothed projection of a moving field calculated by Eq. (3) on the basis of a spectral analysis of the flow pattern recorded at successive instants of time t_i. The velocity of the cylinder was 1.5 m/sec, and the corresponding Reynolds number was $\sim 5 \cdot 10^6$. Figure 2 also shows the values of the variance of the field $\sigma_T^2 = 430$, 670, 960, 1150, 1430, 1250, and 740 mm (curves 1-7, respectively, where the numbers on the curves correspond to successive instants t_i with $i = 1$-7).

The data on the variation of the spectrum show that as turbulence develops, there is an increase in the relative intensity of the low-frequency components, which can be accounted for by an increase in the scales of dense inhomogeneities. After a certain time the general decrease of spectral amplitudes corresponds to the scattering of turbulent energy into the surrounding medium during the final stages of the flow. A comparison of the curves for times t_2 and t_7 shows that at these times the values of the variance are nearly the same, but the differences in the behavior of the curves indicate the transfer of energy to a lower frequency region for developed turbulence. These conclusions are confirmed by the general concepts of the development of turbulent flow [8]. Thus, the use of optical instruments employing photographic recording for investigating the microstructure of a moving field and the spectral analysis of projections of the field recorded at successive instants permit a quantitative estimate of the variation of the field during the motion.

LITERATURE CITED

1. P. Bradshaw, An Introduction to Turbulence and Its Measurement, Pergamon, New York (1971).
2. S. S. Kutateladze, Boundary Layer Turbulence [in Russian], Nauka, Novosibirsk (1973).
3. V. N. Stasenko, "Application of a shadow instrument for determining turbulence characteristics," Zh. Prikl. Mekh. Tekh. Fiz., No. 3 (1970).
4. G. D. Salamandra, Photographic Methods for Studying High-Speed Flows [in Russian], Nauka, Moscow (1974).
5. K. V. Konyaev, Spectral Analysis of Random Processes and Fields [in Russian], Nauka, Moscow (1973).
6. N. S. Shestov, Separation of Optical Signals from a Background of Random Disturbances [in Russian], Sov. Radio, Moscow (1967).
7. V. F. Zakharenkov, R. P. Filimonov, and A. S. Pavlyuchuk, "The microphotometric method of analyzing photographic noise," Opt.-Mekh. Prom-st', No. 3 (1973).
8. J. O. Hinze, Turbulence, McGraw-Hill, New York (1959).
9. S. Chandrasekhar, Hydrodynamic and Hydromagnetic Stability, Oxford University Press (1961).
10. J. Bendat and A. Piersol, Measurement and Analysis of Random Data, Wiley, New York (1966).